Engineering the Active Phase in Ni-BDC via Cr Doping and Electrochemical Reconstruction for Efficient Methanol Oxidation

Haoshan Hong, Qianqian Zhong, Haonan Li, Qijing Bu* and Qingyun Liu*

College of Chemical and Biological Engineering, Shandong University of Science and Technology, Qingdao 266590, China

E-mail: Bu-qijing@sdust.edu.cn; qyliu@sdust.edu.cn

Experimental Section

NiCr-BDC was prepared via a typical hydrothermal method according to the previously reported literature.[1] In detail, nickel foam (1 cm × 0.75 cm × 0.8 mm) was sonicated in 3 M hydrochloric acid solution for 5 min, and rinsed thoroughly with ultrapure water and anhydrous ethanol in sequence until the surface became neutral. The pretreated nickel foam (NF) was added into a 30 mL Teflon-lined containing a homogeneous mixture of $Ni(CH_3COOH)_2$ (0.2239 mg), $CrCl_3$ (0.0266 mg), 1,4-terephthalic acid (0.0830 mg), ultrapure water (7.5 mL), and N,N-dimethylacetamide (DMAC, 7.5 mL). The autoclave was then sealed and heated at 150 ˚C for 10 h to fabricate CrNi-BDC nanocrystals grown on the NF surface. After natural cooling to room temperature, the as-prepared CrNi-BDC/NF composite was thoroughly rinsed with ultrapure water and ethanol for several times, followed by vacuum drying at 60°C. For comparison, Ni-BDC was prepared using the same procedure except without the addition of $CrCl_3$.

Electrochemical Measurements

All electrochemical measurements were performed on a CHI760E electrochemical workstation (Chenhua, China) using a three-electrode system. The obtained CrNi-BDC/NF and Ni-BDC/NF were directly used as working electrode without any further modification. A saturated Ag/AgCl electrode and a platinum foil (1 cm × 1 cm) were served as the reference electrode and counter electrode, respectively. All electrochemical measurements related to the voltage determination were calibrated with respect to the reversible hydrogen electrode (RHE) according to the following

equation: E (vs. RHE) = E + E (vs. Ag/AgCl) + 0.059 × pH. The performance of methanol oxidation reaction (MOR) performance was evaluated by CV and LSV with a voltage range of 1V-1.6 V vs. RHE at a scan rate of 0.05 V s^{-1} using a N_2 saturated 1 M KOH + 1 M CH_3OH solution as the electrolyte. The oxygen evolution reaction (OER) performance was evaluated in a 1 mol L^{-1} KOH solution. Electrochemical impedance spectroscopy (EIS) measurement was performed at a constant voltage of 1.4 V vs. RHE. The I-T test was carried out at a constant voltage of 1.6 V vs. RHE. The CV cycle stability was assessed by conducting 500 CV cycles within the voltage range of 1-1.6 V vs. RHE. The C_{dl} value was obtained via CV curves at different scan rates (0.01, 0.02, 0.03, 0.04, 0.05, 0.06, 0.07, 0.08, 0.09 and 0.1 V s^{-1}).

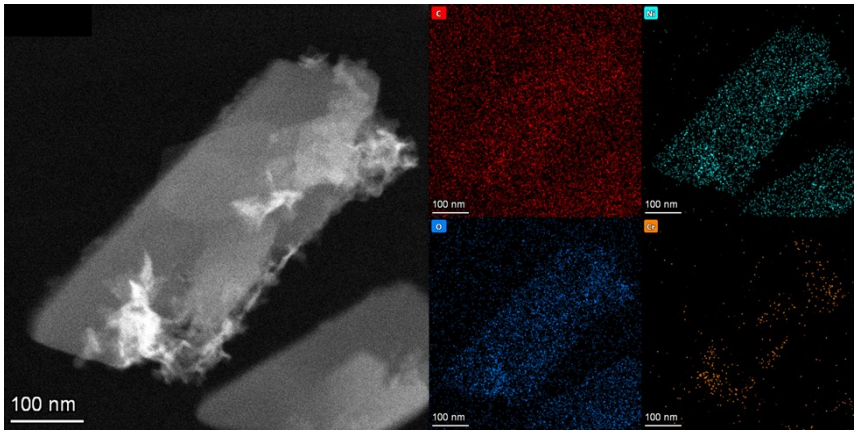

Figure S1. EDS mapping images of CrNi-BDC.

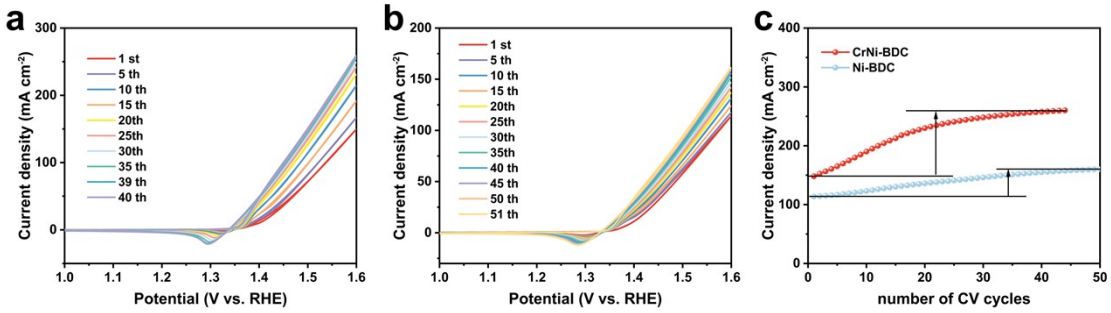

Figure S2. CV cycles test of CrNi-BDC (a) and CrNi-BDC (b), and (c) Current density of CrNiBDC and Ni-BDC at 1.6 V with sustaining CV cycles.

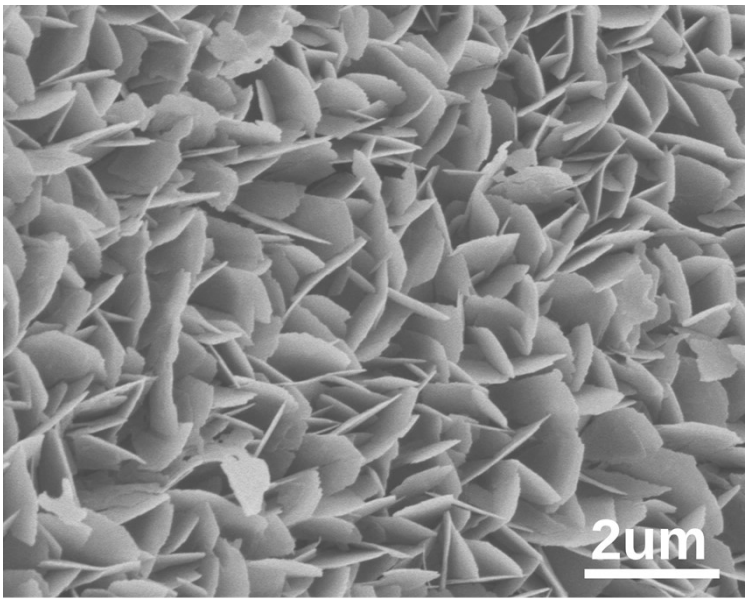

Figure S3. SEM image of R-Ni-BDC.

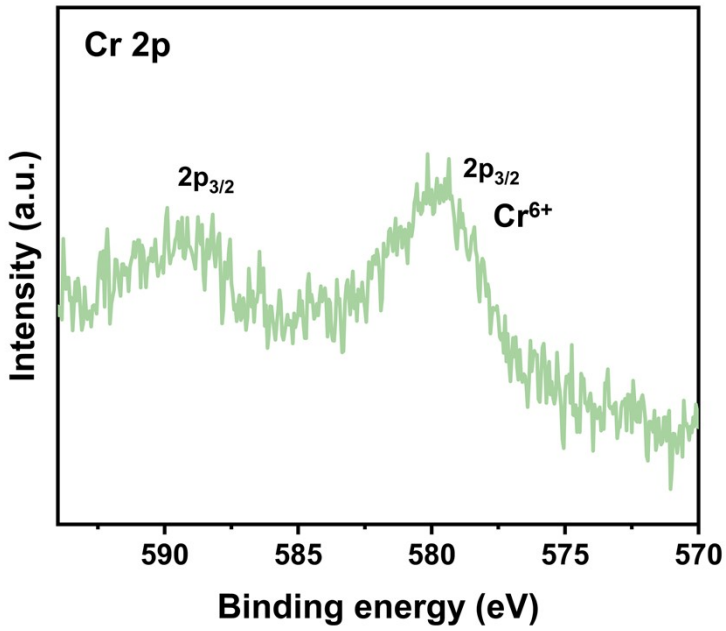

Figure S4. Cr 2p XPS spectra of R-CrNi-BDC.

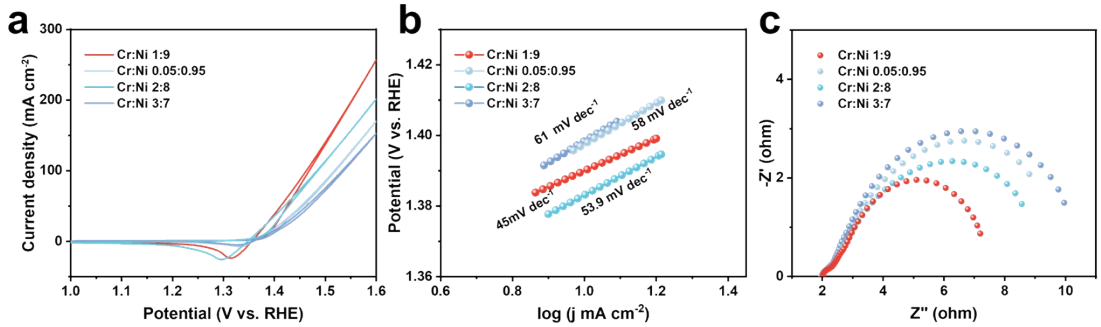

Figure S5. (a) CV curves, (b) Tafel plots, (c) Nyquist plots of Cr:Ni (0.05:0.95, 1:9, 2:8 and 3:7) electrocatalyst in 1M KOH + 1 M CH_3OH solution at a scan rate of 50 mV s^{-1}.

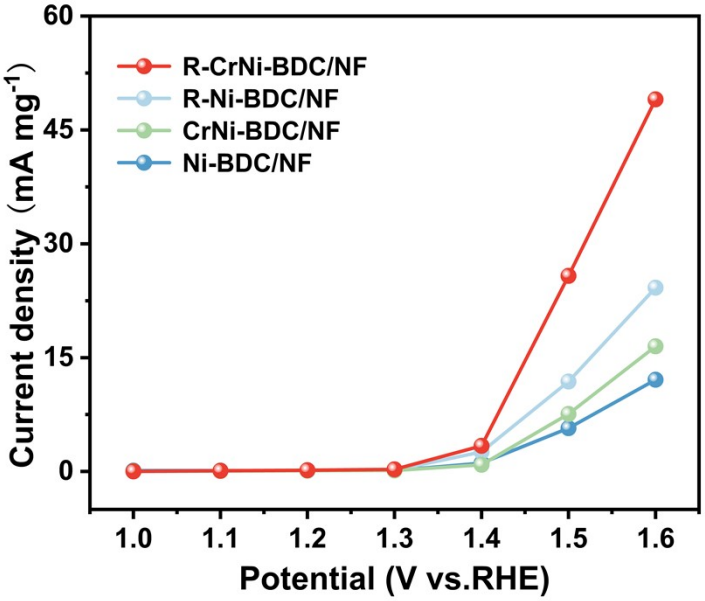

Figure S6. The mass activity of R-CrNi-BDC, R-Ni-BDC, CrNi-BDC and Ni-BDC.

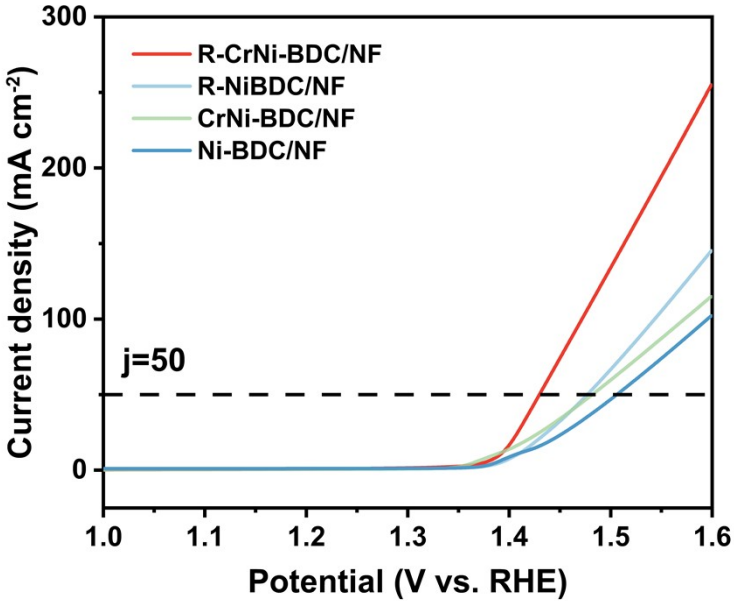

Figure S7. LSV curves of R-CrNi-BDC, R-Ni-BDC, CrNi-BDC and Ni-BDC.

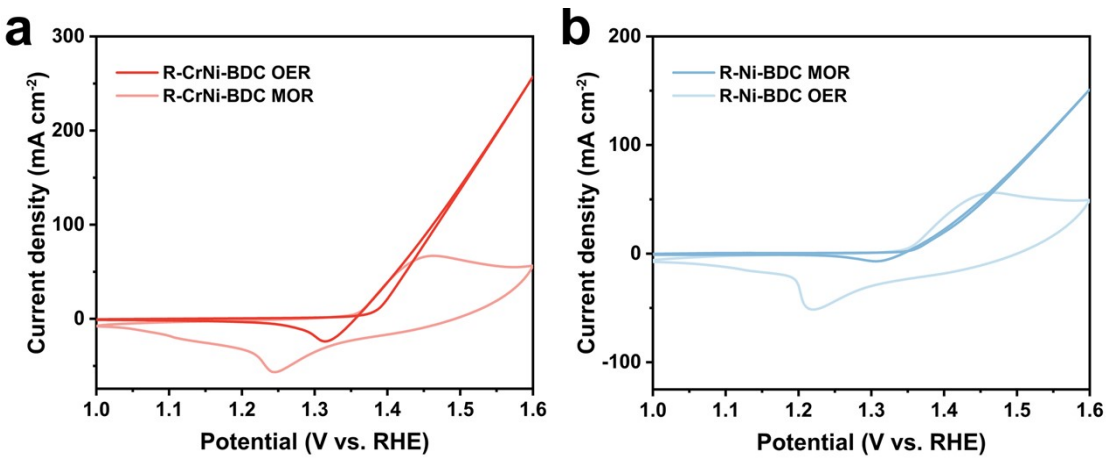

Figure S8. CV curves of R-CrNi-BDC and R-Ni-BDC electrocatalyst in KOH with and without CH_3OH solution at a scan rate of 50 mV s^{-1}.

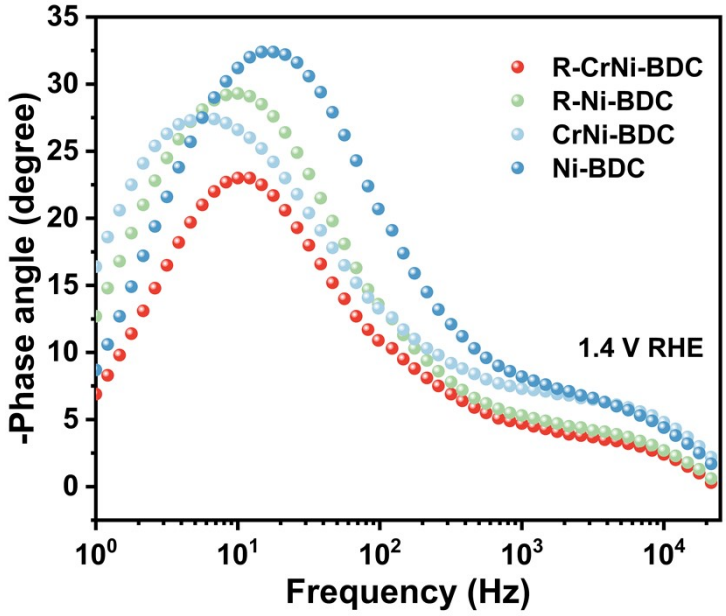

Figure S9. Bode plot of R-CrNi-BDC, R-Ni-BDC, CrNi-BDC and Ni-BDC.

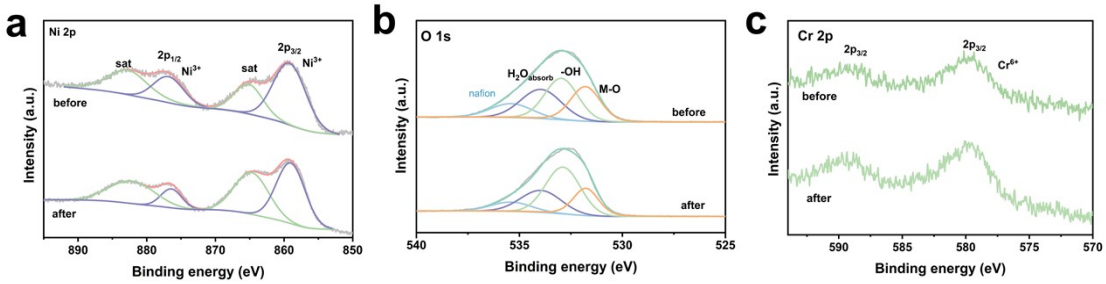

Figure S10. (a) Ni 2p, (b) O 1s, (c) Cr 2p XPS spectra before and after stability test of R-CrNi-BDC.

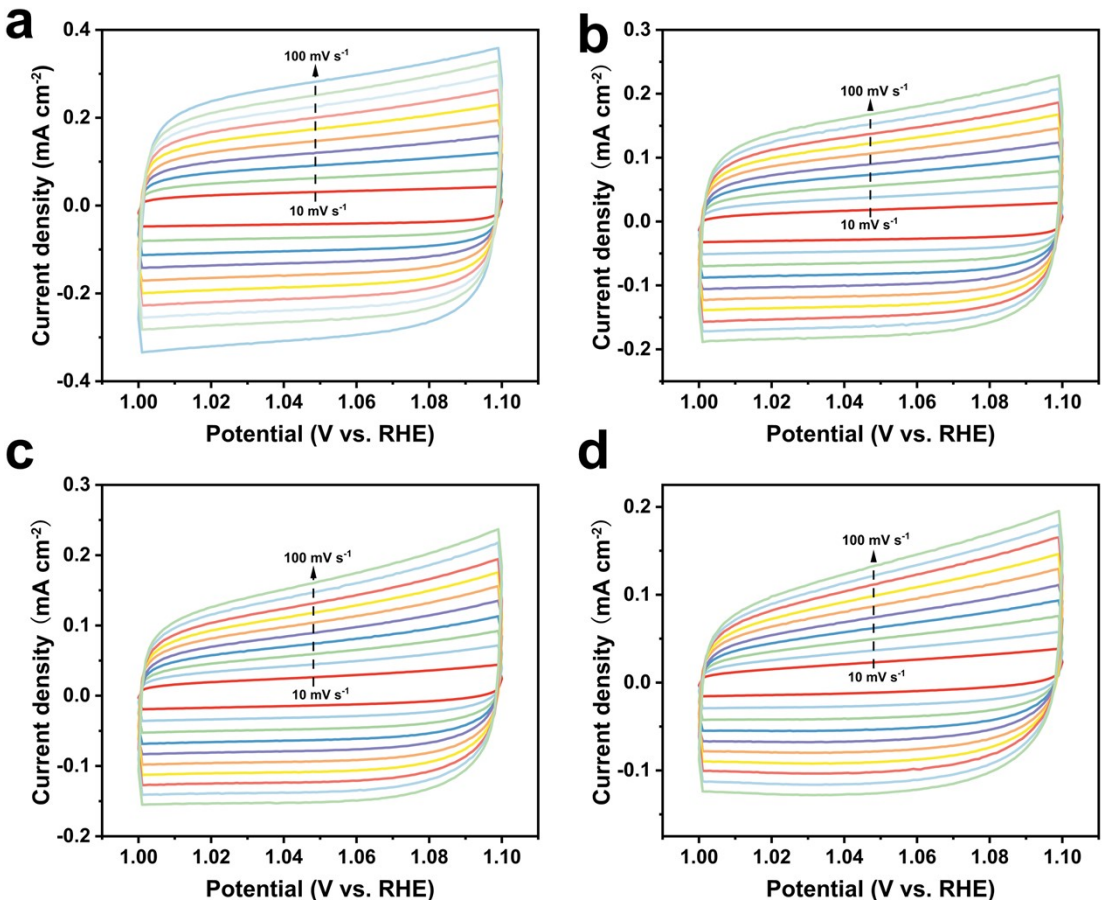

Figure S11. Cyclic voltammetry curves of (a) R-CrNi-BDC, (b) R-Ni-BDC, (c) CrNi-BDC and (d) Ni-BDC in 1.0 M KOH solution.

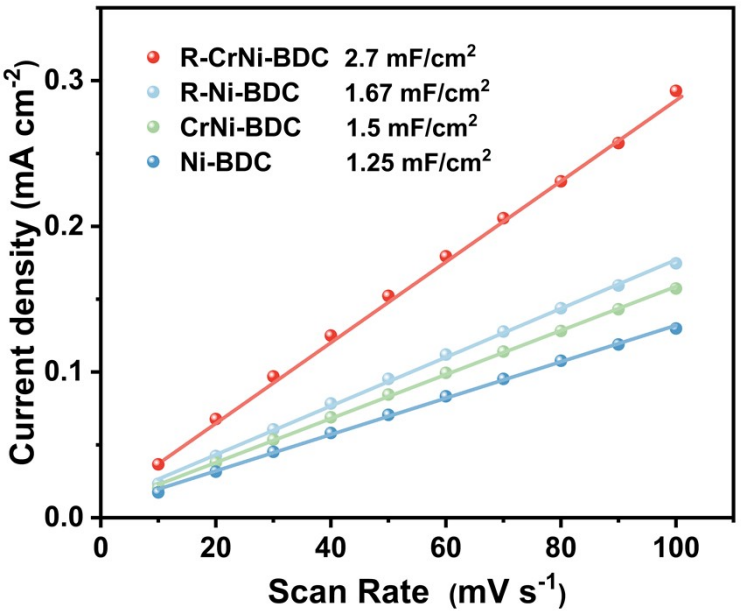

Figure S12. Liner fitting of scanning rate and current density.

Table S1. The fitted results of Nyquist plots for R-CrNi-BDC, R-Ni-BDC, CrNi-BDC and Ni-BDC electrocatalyst.

catalyst	$R_1(\Omega)$	$R_{ct}(\Omega)$	CPE_1 (F cm^{-2})
R-CrNi-BDC	2.564	5.079	9.8×10^{-3}
R-Ni-BDC	2.476	9.715	9.4×10^{-3}
CrNi-BDC	2.844	12.4	1.3×10^{-3}
Ni-BDC	2.6	13.72	4.9×10^{-3}

Table S2. The electrochemical performance of R-CrNi-BDC, R-Ni-BDC, CrNi-BDC and Ni-BDC electrocatalyst.

catalyst	Current Density (mA cm^{-2}) at 1.6 V vs. RHE	Mass activity (mA mg^{-1}) at 1.6 V vs. RHE	Charge Transfer Resistance (Ω)	Tafel Slope (mV dec^{-1})
R-CrNi-BDC	257.4	49	5.079	45
R-Ni-BDC	142.8	24.2	9.715	68
CrNi-BDC	160	16.4	12.4	72
Ni-BDC	103.8	12	13.72	89

References

1. Bao, Y. ,Ru, H. ,Wang, Y., et al., Hetero MOF-On-MOF of Ni-BDC/NH_2-MIL-88B(Fe) Enables Efficient Electrochemical Seawater Oxidation. *Advanced Functional Materials* **2024,** *34* (22), 2314611.

2. Ning, M. ,Wang, Y. ,Wu, L., et al., Hierarchical Interconnected NiMoN with Large Specific Surface Area and High Mechanical Strength for Efficient and Stable Alkaline Water/Seawater Hydrogen Evolution. *Nano-Micro Letters* **2023,** *15* (1), 157.

3. Chen, M. ,Zhang, Y. ,Chen, J., et al., In Situ Raman Study of Surface Reconstruction of FeOOH/Ni_3S_2 Oxygen Evolution Reaction Electrocatalysts. *Small* **2024,** *20* (23), 2309371.